Current Research (2002) Newfoundland Department of Mines and Energy
Geological Survey, Report 02-1, pages 53-65

A STUDY OF THE METAMORPHIC AUREOLE OF THE MOUNT PEYTON INTRUSIVE SUITE, DUNNAGE ZONE, CENTRAL NEWFOUNDLAND

G.F. Hynes[1] and T. Rivers
Department of Earth Sciences, Memorial University of Newfoundland
St. John's, Newfoundland, A1B 3X5

ABSTRACT

The Late Ordovician to Early Silurian Badger group, located in the Dunnage Zone, central Newfoundland, and consisting mainly of low-grade sandstone and pelite, is host to the post-kinematic, polyphase Mount Peyton Intrusive Suite. In the Rattling Brook transect, the Mount Peyton Intrusive Suite consists of four main phases, from oldest to youngest these are: pyroxene–hornblende gabbro, quartz diorite–granodiorite, biotite granite and biotite–hornblende granite. Dykes of various compositions are also contained within the suite. Previous workers suggested the Mount Peyton Intrusive Suite is a batholith; however, on the basis of field relationships observed in the study area, the intrusion is inferred to be a sheet-like body or laccolith, 1 to 2 km thick, where its lower contact is parallel to bedding in the metasediments of the Badger group.

Emplacement of the Mount Peyton Intrusive Suite as a laccolith resulted in metamorphism of pelites in the Badger group and formation of a contact aureole on the underside of the intrusion. Hornfels near the intrusive contact, contain the maximum phase assemblage: hypersthene–cordierite–biotite–alkali feldspar–plagioclase–quartz–magnetite–ilmenite.

Mineral analyses were obtained using an electron microprobe from a representative, low-variance sample in the aureole for the purpose of geothermobarometry. Multi-equilibrium calculations provide a well-constrained quantitative maximum temperature and pressure estimate of 810°C and 2.5 kbar for rocks situated 170 m below the intrusive contact. These P–T conditions are in good agreement with a qualitative estimate using petrogenetic grids. Based on the absence of partial melting in pelites with the sub-assemblage quartz–alkali feldspar–plagioclase, for which a metamorphism temperature of 810°C was obtained, it is inferred that a_{H2O} in the aureole in the Rattling Brook transect was between $0.5 < a_{H2O} < 1$.

To the authors' best knowledge, this is the first report of a granulite-facies assemblage in a thermal aureole in the Paleozoic rocks of the Newfoundland Appalachians.

INTRODUCTION

The purpose of this study is to describe the aureole of the Mount Peyton Intrusive Suite (MPIS) along a transect in Rattling Brook and to determine the metamorphic conditions responsible for its development. The estimation of P, T, X_{H2O} conditions is based on mineralogical evidence from samples taken across the aureole.

The Rattling Brook transect is located on NTS map area 2E/03 between 49°00' N and 49°05' N and 55°15'W and 52°20' W. It lies about 15 km east of Bishop's Falls between the Trans-Canada Highway (TCH) and Norris Arm (Figure 1).

The study area lies within the Exploits Subzone of the Dunnage Zone in central Newfoundland and is mainly underlain by rocks of the Badger group. Here, the Badger group consists of green and grey thin- to medium-bedded, cleaved, locally fossiliferous greywacke that form as hornfels in the units of the MPIS (Dickson, 1994).

Large Silurian and Devonian composite intrusions that have granite phases that cut mafic phases are characteristic

[1] Present address: Department of Geological Sciences, Queen's University, Kingston, Ontario, Canada

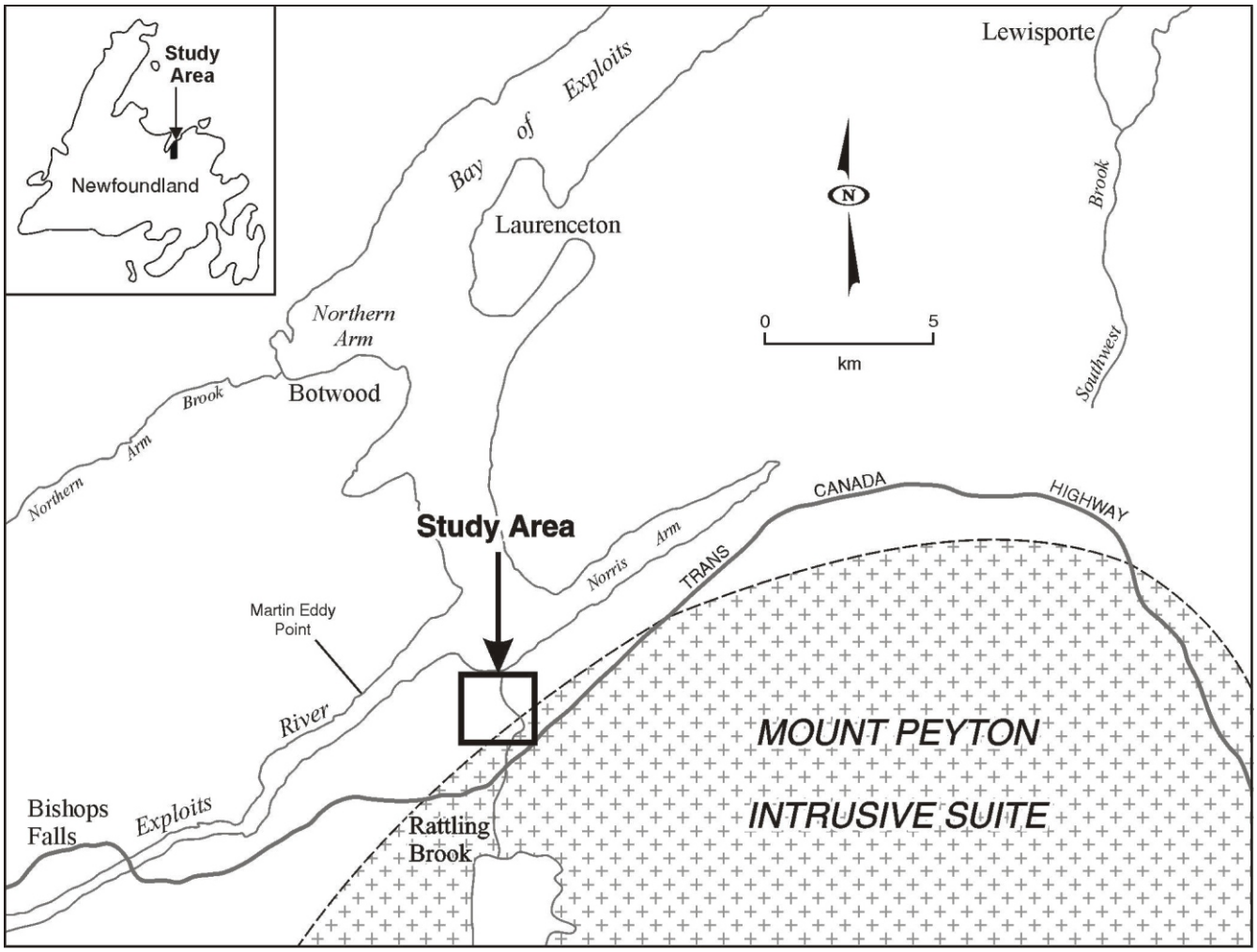

Figure 1. *Location of the study area, central Newfoundland.*

of the Exploits Subzone (Williams *et al.,* 1988). The aureole of one of these intrusions, the MPIS, is the focus of this study. The 1400 km^2 MPIS consists predominantly of fine-grained, grey, equigranular, massive gabbro and diorite with subordinate medium- to coarse-grained gabbro. Medium-grained granodiorite to granite veins, dykes and plugs are common in the gabbro (Dickson, 1994).

PREVIOUS WORK

THE MOUNT PEYTON INTRUSIVE SUITE

The MPIS is a large composite plutonic body that intrudes the Early Silurian rocks of the Badger group in the Rattling Brook area, central Newfoundland (Dickson, 1994). It is Late Silurian and has been dated at 424 ± 2 Ma (U–Pb zircon, G.R. Dunning, unpublished data, 1994). It ranges in composition from pyroxene–hornblende gabbro to biotite granite. The body is exposed south of the Trans-Canada Highway between Bishop's Falls and Glenwood.

Williams (1962) was the first to outline the large gabbroic body south of Norris Arm when he produced the first 1:250 000-scale map of the area. The large gabbroic body was termed the Mount Peyton Batholith, a name that was later changed to MPIS by Blackwood (1982). A regional lithogeochemical survey on the MPIS was conducted by Strong *et al.* (1974), who concluded that the gabbro was derived from a mantle source, whereas the associated granite resulted from partial melting of the crust as a result of the advected heat from the mafic magma. The Ar–Ar dating by Reynolds *et al.* (1981) indicated a Late Silurian age (420 Ma) for the gabbro of the MPIS. The petrographic character of the intrusive rocks in the study area was described by Dickson (1994) and a 1:50 000-scale map of NTS map area 2D/03 was produced by Dickson *et al.* (2000).

COUNTRY ROCKS

Murray and Howley (1881) carried out the first survey work in the study area in 1871. They noted various coral,

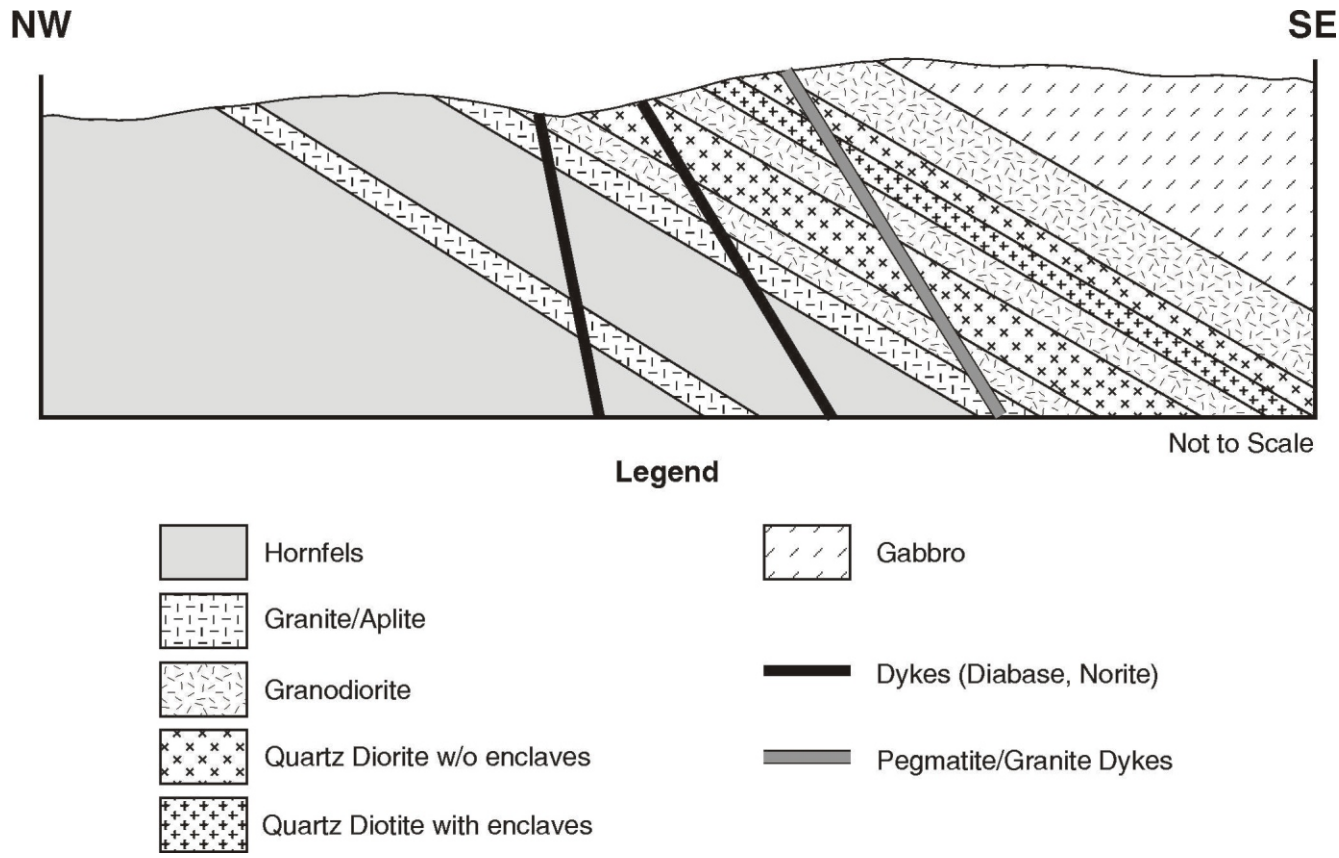

Figure 2. *Schematic cross-section of the field area showing the contact relationships observed along the Rattling Brook traverse.*

crinoid, brachiopod and trilobite fossils in the conglomerates at 'Martin Eddy Point' (Figure 1). These fossils were examined by Billings (1865) of the Geological Survey of Canada who inferred that they were of Llandoverian (Early Silurian) age. The fossiliferous conglomerate described by Murray and Howley (1881) was assigned to the Goldson Formation. Subsequent work by Dean (1977) resulted in the Goldson Formation being removed from the Botwood Group. Williams *et al*. (1995) included the Goldson Formation in the informally named Badger group.

Kalliokoski (1953) was the first to describe hornfels around Norris Arm while conducting a regional survey to assess mineral potential in the area. Field relationships among the stratified units were also described by Dickson (1994) and displayed on a 1:50 000-scale map (NTS map area 2D/03; Dickson *et al.*, 2000).

FIELD RELATIONSHIPS

The 1400 km^2, multiphase MPIS forms a large oval-shaped body that is approximately 38 km east–west by 62 km wide north–south.

In this study, the MPIS has been divided into four lithological units. These units are: pyroxene–hornblende gabbro, quartz diorite–granodiorite, biotite granite, and biotite–hornblende granite. Several of these units individually demonstrate more than one intrusive episode. In addition, several dyke suites of various compositions occur. A relative order of emplacement can be determined for some of the units, but the entire chronology could not be unambiguously determined due to the local geological complexity and limited size of the field area. Inferences concerning the shape and dimensions of the intrusions are also addressed in this section, and related to the order of emplacement of the suite.

Field relationships observed in this study between the hornfels and the granitic unit indicate that the sediments of the Badger group dip shallowly under the MPIS, suggesting that the latter is a sheet-like body and laccolithic in shape. Figure 2 is a schematic cross-section of the contact relationships observed in the field area. The average dip of the sediments beneath the laccolith is 35°.

The body in the study area comprises several sheet-like intrusions. The granite and quartz diorite–granodiorite units occur adjacent to the pyroxene hornblende gabbro as subhorizontal sheets that dip gently to the southeast, indicating multiple intrusive events were involved in the formation of the laccolith. Dickson (1994) described similar features along the gabbro contact close to the TCH.

ORDER OF EMPLACEMENT

In the study area, the pyroxene–hornblende gabbro is not seen in contact with any of the other units so its relationship in the sequence has to be inferred (*see below*). Field relationships indicate more than one episode of emplacement of the quartz diorite–granodiorite unit. Plate 1 shows a phase of the quartz diorite–granodiorite unit containing enclaves (A) cut by another phase of the same composition having aligned enclaves (B). Note that the enclave at the bottom of the photo is cut by the younger phase. The enclaves in the younger phase display a flow foliation aligned toward 152°. The flow foliation suggests that the sheets were emplaced by flow from the centre of the intrusion in a direction perpendicular to the intrusive contact. Evidence for several episodes of emplacement of the quartz diorite–granodiorite unit is also shown in Plate 2.

In this case (Plate 2), a finer grained unit (A) is intruded by a coarser grained unit having abundant enclaves (C). The petrography of all these units indicates a similar composition, thus observed contact relations within this unit indicate at least three different magma pulses and a multiple emplacement history is inferred.

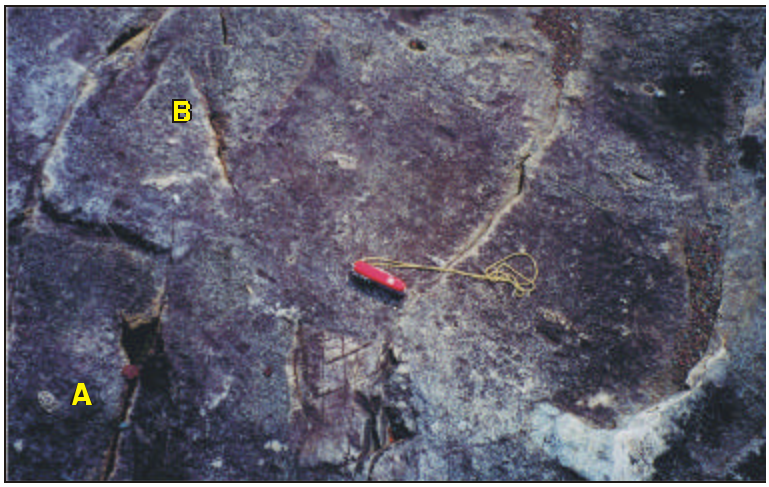

Plate 1. *Field photograph of the quartz diorite–granodiorite unit (A) cut by another phase of quartz diorite–granodiorite with aligned enclaves (B). The enclaves are oriented toward 152°.*

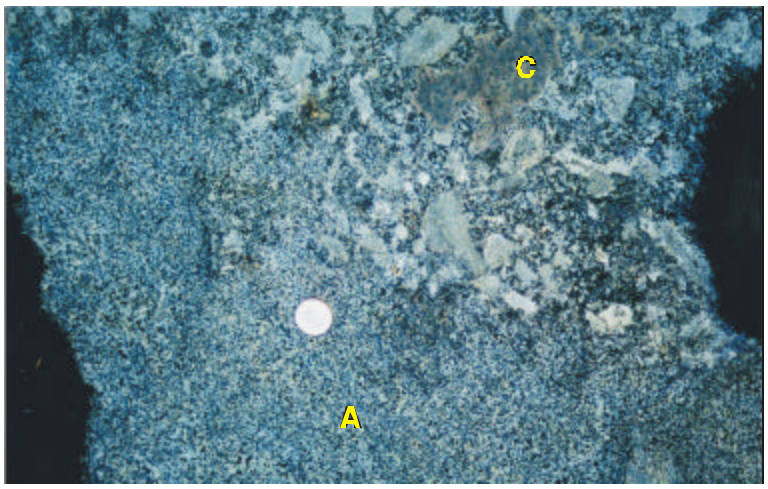

Plate 2. *Field photograph of a fine-grained quartz diorite (A) intruded by a coarser grained quartz diorite with abundant enclaves (C).*

The biotite granite unit was observed to intrude the quartz diorite–granodiorite unit in a number of areas, indicating that it is younger. In addition, the granite is seen to cut and contain inclusions of hornfels, indicating that it was emplaced later.

Contact relations between the biotite–hornblende granite and the other igneous phases in the sequence were not determined. However, on the basis of intrusive relationships with the hornfels, the unit was emplaced after the formation of the hornfels. Thus, it is inferred that the biotite–hornblende granite was emplaced at approximately the same time as the biotite granite unit.

On the basis of the observations noted above, it is possible to infer the relative chronology of the pyroxene–hornblende gabbro in the intrusive sequence. In so doing, the following assumptions are made: i) that the pyroxene–hornblende gabbro was the most mafic, and therefore presumably the hottest magma in the MPIS; and ii) that the hornfels was developed as a result of emplacement of the pyroxene–hornblende gabbro. With these assumptions, the order of emplacement of the major components of the MPIS is pyroxene–hornblende gabbro, followed by quartz diorite–granodiorite, followed by the two granitic units.

In addition to the major phases of the MPIS, there are several minor associated phases including pegmatitic–granitic dykes and mafic dykes in the study area; quartz veining is locally abundant in the field area.

CONTACT AUREOLE

The aureole rocks of the MPIS have a relatively simple structural history and have a single fabric preserved in most samples. The aureole is developed in rocks of pelitic to semipelitic composition that are part of the structurally underlying Badger group. The metasedimentary rocks consistently strike northeast and vary in dip from 20 to 50° toward the southeast. The petrographic study of the metapelites was focused on hornfels samples collected along a transect across the aureole. The samples are very fine grained and the use of a transmitting–reflecting light microscope was necessary to determine mineral assemblages.

Four metamorphic mineral assemblages were used to provide an interpretation of the evolution of the aureole. The assemblages are:

A) orthopyroxene–biotite–alkali feldspar–plagioclase–quartz–magnetite–ilmenite;

B) orthopyroxene–cordierite–biotite–alkali feldspar–plagioclase–quartz–magnetite–ilmenite;

C) cordierite–muscovite–biotite–plagioclase–quartz ± magnetite ± ilmenite; and

D) biotite–muscovite–chlorite–quartz–calcite–epidote–plagioclase ± magnetite ± ilmenite.

Assemblage A occurs closest to the contact with the laccolith and therefore is assumed to have been the hottest. Similiarly, assemblage D is farthest from the contact, contains chlorite and muscovite in the absence of alkali feldspar and is considered to be the lowest (oldest) grade. Figure 3 schematically shows the AFM phase relations of assemblages A, B, C, and D in the aureole.

ASSEMBLAGE A

Assemblage A is composed of orthopyroxene–biotite–alkali feldspar–plagioclase–quartz–magnetite–ilmenite. Assemblage A in Figure 3 schematically shows the positions of the stable phases on an AFM diagram projected through alkali feldspar. The assemblage is characteristic of samples taken 10 to 15 m from the contact of the igneous body. Orthopyroxene occurs as subhedral porphyroblasts and very small anhedral grains (Plate 3).

Biotite comprises 50 to 60 percent of the sample and displays a preferred orientation. The SEM imaging of the alkali feldspar revealed the presence of very fine-grained perthitic exsolution.

ASSEMBLAGE B

Assemblage B consists of orthopyroxene–cordierite–biotite–alkali feldspar–plagioclase–quartz–magnetite–ilmenite and corresponds to samples that occur 250 to 300 m from the contact. Assemblage B in Figure 3 shows the stable mineral assemblage plotted on an AFM diagram projected through alkali feldspar. Cordierite occurs as porphyroblasts having inclusions of quartz (Plate 4) and zircon–monazite that display pleochroic yellow haloes due to lattice damage caused by radiogenic decay.

Orthopyroxene grains are very small, subhedral and occur in close proximity to biotite and cordierite. Biotite displays a weak preferred orientation.

ASSEMBLAGE C

Assemblage C is composed of cordierite– muscovite–biotite–plagioclase–quartz ± magnetite ± ilmentite. The presence of stable muscovite and the absence of alkali feldspar and orthopyroxene indicate that this sample is a lower grade assemblage than that of A or B. Assemblage C corresponds to samples taken from locations greater than 400 m from the contact of the MPIS. Assemblage C in Figure 3 schematically shows the stable minerals plotted on an AFM diagram projected through muscovite.

Cordierite occurs as porphyroblasts with inclusions of quartz in assemblage C. The cordierite grains in this assemblage only rarely display pleochroic yellow haloes, in contrast to those in assemblage B, and are commonly difficult to distinguish from plagioclase. Muscovite grains occur as thin subhedral blades and lack a preferred orientation, and biotite forms radially around Fe–Ti oxides.

ASSEMBLAGE D

Assemblage D consists of biotite–muscovite–chlorite–quartz–calcite–epidote–plagioclase ± magnetite ± ilmenite. The presence of chlorite with muscovite indicates that this sample formed under greenschist-facies conditions and is the lowest grade assemblage observed; the assemblage corresponds to samples taken from greater than 600 m from the contact. Assemblage D in Figure 3 schematically shows the positions of the stable phases on an AFM diagram projected through muscovite. All phases in assemblage D occur as small anhedral grains.

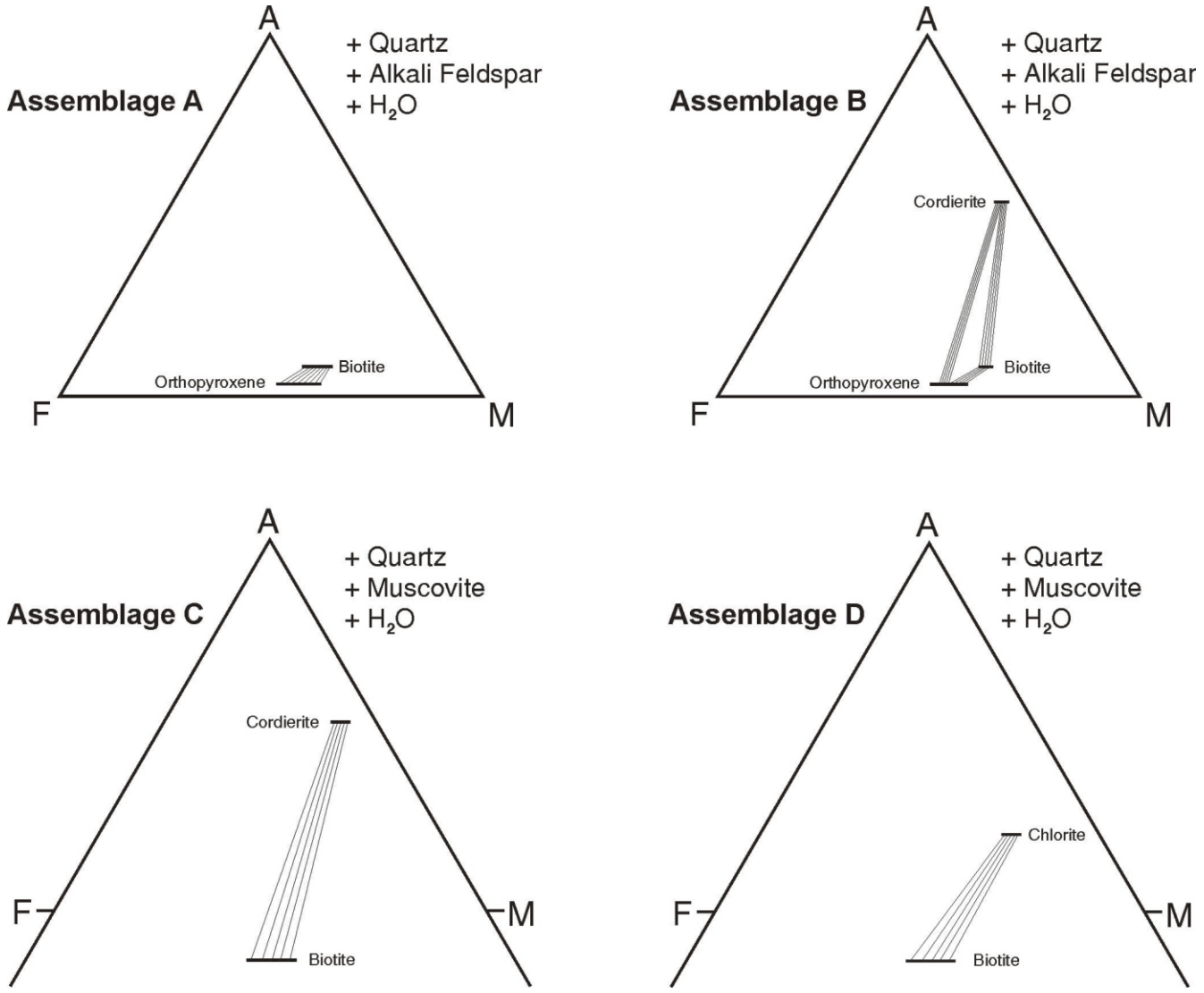

Figure 3. *Schematic AFM diagrams of assemblages A, B, C, and D.*

PRESSURE–TEMPERATURE ESTIMATE

Relative pressure and temperature conditions of each assemblage can be plotted on a schematic KFASH diagram (Figure 4).

Assemblages A and B occur to the right of the orthopyroxene-forming reaction. Furthermore, the lack of migmatitic textures in these samples suggests that they formed at a lower temperature than the granite minimum melting curve. Assemblage C lies between the chlorite and the muscovite breakdown reactions and assemblage D occurs to the left of the chlorite breakdown reaction.

Pattison and Tracy (1991) proposed four facies series types to describe contact aureoles in metapelites. The facies series are numbered from the lowest pressures and include several sub-types. The presence of the sub-assemblage Opx–Crd–Kfs, and the absence of garnet at the highest grades, suggest that conditions most closely resemble facies series 1a of Pattison and Tracy (1991). Facies series 1 corresponds to bathozone 1, close to the boundary with bathozone 2 on Carmichael's (1978) diagram for metapelites. This implies that the pressures in the aureole were less than 2.25 kbar. The absence of Al_2SiO_5 minerals is due to inappropriate (Al-poor) bulk compositions. A temperature estimate cannot be made using Carmichael's (1978) bathozone diagram, although the presence of orthopyroxene implies granulite-facies conditions.

Inspection of a schematic isobaric $T–X_{Fe-Mg}$ diagram for facies series 1a (Figure 5; Pattison and Tracy, 1991) indi-

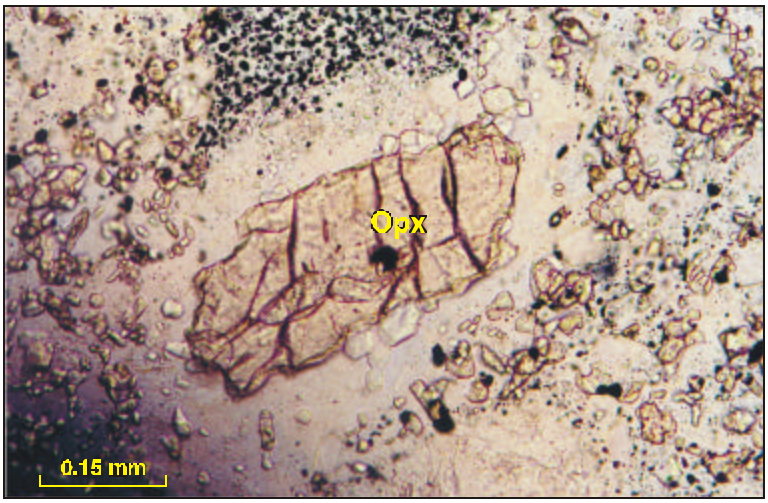

Plate 3. *Photomicrograph of orthopyroxene porphyroblast (PPL, 20X).*

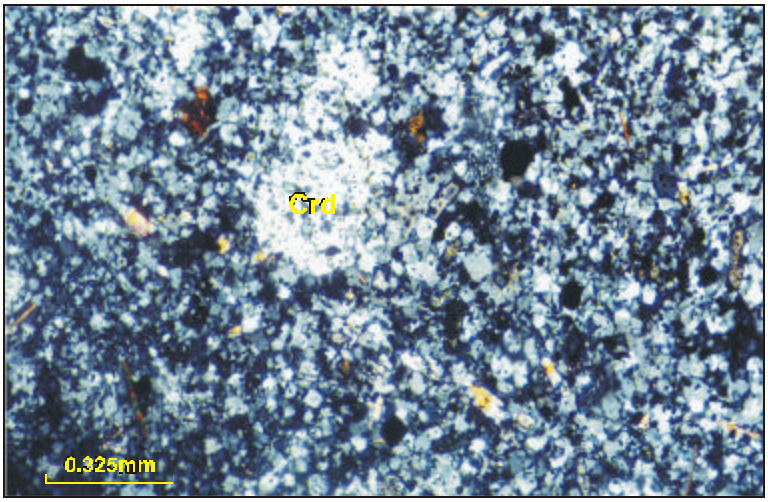

Plate 4. *Photomicrograph of cordierite porphyroblast (XPL, 10X).*

cates that orthopyroxene-bearing assemblages occur at temperatures greater than 750 °C, with first orthopyroxene forming according to the reaction:

$$Bt + Crd + Qtz \Leftrightarrow Opx + Kfs + L \text{ (or } H_2O)$$

where: Bt - biotite, Crd - cordierite, Qtz - quartz, Opx - orthopyroxene, Kfs - alkali feldspar, L - liquid, H_2O - water

As noted above, evidence for melting (e.g., migmatitic textures) was not observed within the hornfels in the study area, so the dehydration reaction is the more likely.

In conclusion, on the basis of observed mineral assemblages and the P–T grid of Pattison and Tracy (1991), a first-order estimate of pressure less than 2.25 kbar and temperature greater than 750°C can be made for the P–T conditions achieved in the inner aureole. This P–T range corresponds to granulite-facies conditions.

ELECTRON MICROPROBE ANALYSES

Sample GH-00-017B was selected for detailed mineral analyses on the basis of proximity to the igneous body and the low variance mineral assemblage as observed with the use of a transmitting light microscope. This sample has assemblage B minerals composed of orthopyroxene–cordierite–biotite–alkali feldspar–plagioclase–quartz–magnetite–ilmenite.

ORTHOPYROXENE

Orthopyroxene occurs as small (0.01 to 0.30 mm) subhedral, unzoned grains. The microprobe analyses of orthopyroxene in oxide weight percent and formula units are given by Hynes (2001). The orthopyroxene grains analyzed have an average X_{Mg} of 0.57 and are hypersthene (Deer *et al.*, 1992). Calcium is below detection limit in most assemblages, and Al varies between 0.76 to 1.83 oxide wt.%. The sum of the octahedral cations (Mg+Fe+Ca+Mn) is slightly less that 2 in most analyses. Similarly, the number of Si ions in tetrahedral coordination is slightly less than 2. Together, these characteristics suggest that the Al is present in both octahedral and tetrahedral sites as the Al–Opx molecule ($Al^{VI}Al^{IV}O_3$). The Al–Opx is related to enstatite by the Mg–tschermak exchange ($Mg_{-1}Si_{-1}Al^{VI}Al^{IV}$).

CORDIERITE

The results of the microprobe analyses for cordierite are given by Hynes (2001). Cordierite occurs as subhedral porphyroblasts (0.10 to 0.40 mm) containing inclusions of quartz and Fe–Ti oxides. None of the analyzed cordierite grains are zoned and X_{Mg} shows very little variation, averaging 0.76. Cordierite analysis totals add up to 100 percent within analytical error, suggesting that there is no H_2O or CO_2 in the axial channel of the cordierite and that the mineral is anhydrous.

BIOTITE

Biotite grains analyzed are slightly to moderately Mg-rich and have significant differences between samples, ranging from X_{Mg} = 0.64 - 0.60 in GH-00-017B. Biotites in GH-00-017B are deficient in Si and Al^{IV} to fill the tetrahedral (Z) sites, and the remaining tetrahedral sites are filled with Ti. The low octahedral Al is compatible with the absence of an Al-saturating phase (Al_2SiO_5) in the analyzed samples. Minor Cl is present in all biotites for which it was analyzed (*see* Hynes, 2001).

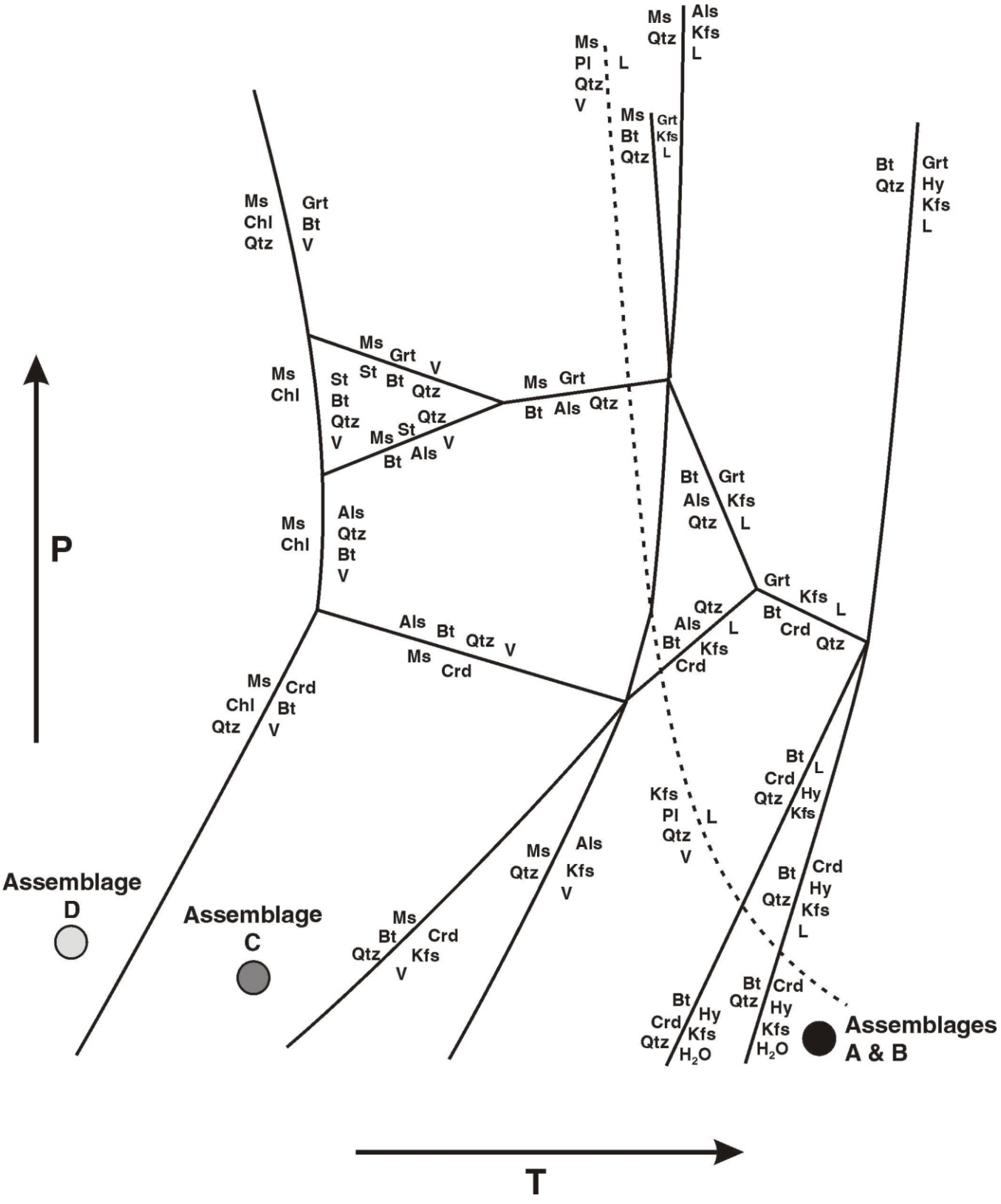

Figure 4. *Schematic P-T diagram for the KFASH system showing relative positions of assemblages A, B, C and D (modified from Pattison and Tracy, 1991).*

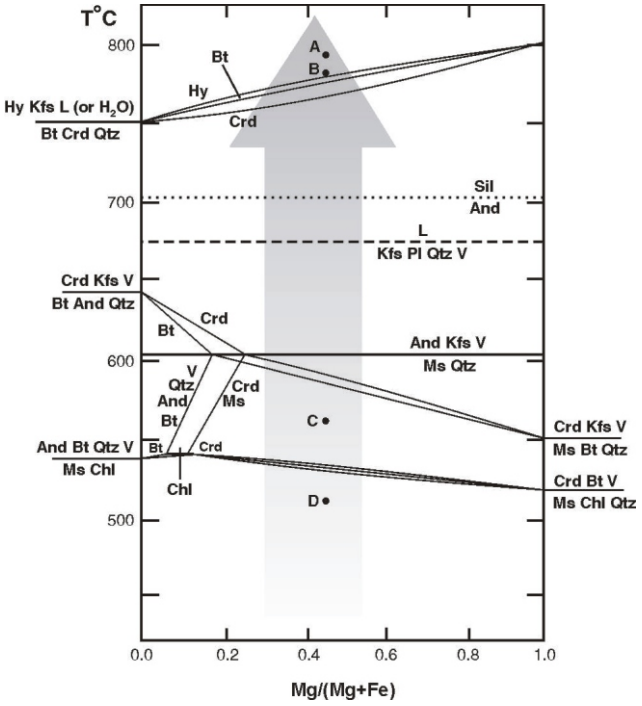

Figure 5. *Schematic isobaric T-X_{Fe-Mg} diagram (modified after Pattison and Tracy, 1991) for facies series 1a showing approximate relative positions of assemblages A, B, C, and D in this study. Note $a_{H2O}=1$.*

ALKALI FELDSPAR

Alkali feldspars in section GH-00-017B display antiperthite exsolution textures. Potassic compositions (X_K = 0.88) are exsolved from host feldspars with more sodic compositions (X_K = 0.39) (*see* Hynes, 2001).

PLAGIOCLASE FELDSPAR

Plagioclase grains are anhedral and are unzoned. Grains in GH-00-017B have an average composition of X_{Na} = 0.53 (*see* Hynes, 2001).

GEOTHERMOBAROMETRY

Thermobarometric calculations were performed using TWQ version 2.02 (Berman, 1991). Sample GH-00-017B was chosen for thermobarometric calculations. This sample is not the closest to the intrusion contact, and therefore cannot be assumed to be the highest grade assemblage. It comes from about 250 to 300 m from the contact. However, it was chosen for analysis due to the presence of a low variance equilibrium assemblage consisting of cordierite–hypersthene– biotite–alkali feldspar–quartz.

As a first step, reactions not involving an H_2O-rich fluid phase were calculated using TWQ. End members for orthopyroxene, cordierite, biotite, alkali feldspar, and plagioclase were entered into the program and appropriate solution models were employed (Berman, 1991).

Thermodynamic calculations using the TWQ database assume that cordierite is anhydrous, which is consistent with inferences from analyses in this study where the total oxide sum for cordierite analyses is 100 percent, within analytical error. The rationale for including aluminous orthopyroxene (aOp) was previously noted. In this study, orthopyroxene contains both octahedral and tetrahedral Al, compatible with the observations of Deer *et al.* (1992), who noted that orthopyroxene can contain up to 0.5 atoms of Al per formula unit in high-grade metamorphic rocks, especially those in the granulite facies. Figure 6 shows the calculated positions of these reactions in P–T space.

From Figure 6, it can be seen that two of the three Fe–Mg exchange geothermometers yielded temperatures in the range of about 750 to 810°C, with the Opx–Bt thermometer yielding a temperature about 50°C higher than the Opx–Crd thermometer. The Crd–Bt geothermometer yielded an impossibly high temperature estimate of about 1400°C, outside the limits of the figure. The lack of precision of this geothermometer is inferred to be due to the small difference in X_{Mg} between coexisting cordierite and biotite. This results in the equilibrium being very sensitive to small analytical errors and to the solution model employed. Intersections of the geothermometers and geobarometers in Figure 6 yield a range of P–T estimates for the assemblage from approximately 4.5 kbar and 750°C to 2.5 kbar and 810°C. In this case, if equilibria involving Fe–Crd are eliminated, the quality of the intersection improves significantly and the remaining 3 equilibria intersect at a single P–T point at approximately 2.5 kbar and 810°C. This pressure and temperature is tentatively taken as the best estimate of the P–T conditions for the sample at the time of hornfelsing, a conclusion that is evaluated in the light of other results, as described below.

The addition of H_2O as a phase allows several more reactions, which can, in principle, be calculated from both Fe and Mg end-members. However, only Mg end-member reactions were used in this study. Figure 7 shows the results of calculations for a_{H2O} = 1 for the fluid present reactions using Mg-rich end members.

Comparison of the results involving Mg–cordierite reactions in Figure 6 with those in Figure 7 indicate excellent agreement, with a single intersection at 2.5 kbar and

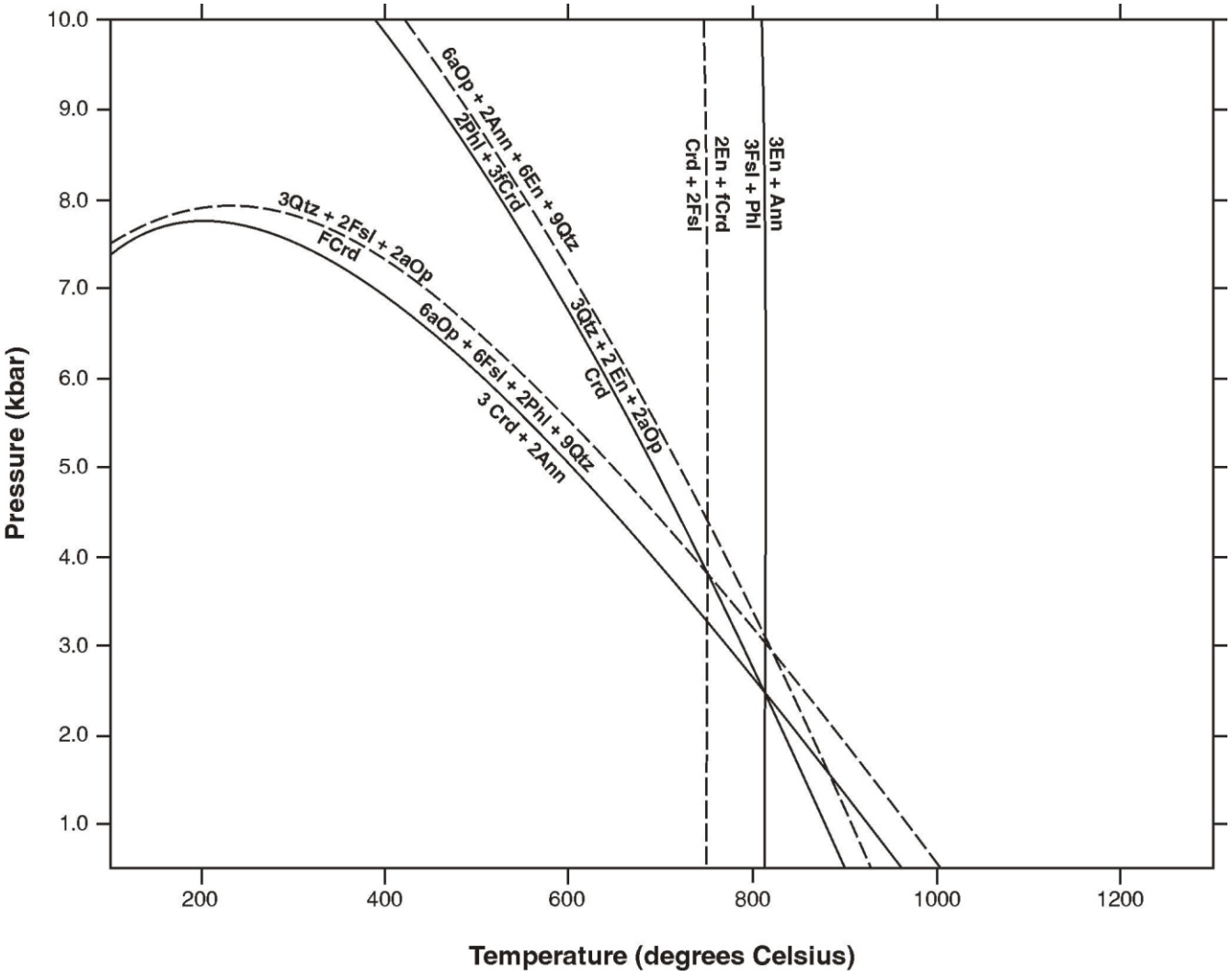

Figure 6. *Positions of the solid-solid reactions in P-T space. Note: dash lines denote reactions calculated using the Fe-cordierite end member.*

810°C. This result suggests that all phases in these reactions are in equilibrium and the solution models are internally consistent.

An approximate estimate can be made for the activity of water (a_{H2O}) in the system. TWQ assumes, unless stated otherwise, that a_{H2O} in the calculations is equal to one. The H_2O present and H_2O absent reactions calculated using TWQ all intersect in a very limited area of P–T space, yielding precise internally consistent pressure and temperature estimates. Since a good intersection is achieved for calculations involving both H_2O conserving and dehydration reactions, it could be inferred that a_{H20} was equal to 1. However, a plot of temperature versus a_{H20} for relevant Mg-cordierite reactions was made to investigate the influence of a_{H20} in the system (Figure 8).

Figure 8 shows that for a variation of a_{H20} from 1 to 0.5, the temperatures of the two equilibria are lowered by <50°C. Thus, the reactions are not sensitive indicators of a_{H2O}, and the coincidence of the P–T intersection for fluid conserving and dehydration reactions does not precisely define a_{H2O} as equal to 1, given reasonable errors in the geothermometric estimates (± 50°C). Therefore, it is concluded that, within the precision of the temperature estimate, a_{H2O} is approximately bracketed between 1 and 0.5. If a_{H2O} were equal to 1, the reaction: An + Kfs + Qtz + H_2O ⇌ Liquid, should have occurred and melting textures should be present in the contact aureole. The absence of anatexis in the field area indicates that a_{H2O} was less than 1. The T-X_{H2O} diagram suggests that X_{H2O} in the granulite facies part of the aureole was between 1 and 0.5. This condition may not apply everywhere in the inner aureole, as Dickson (1994) has observed migmatites in southwest portion of the study area.

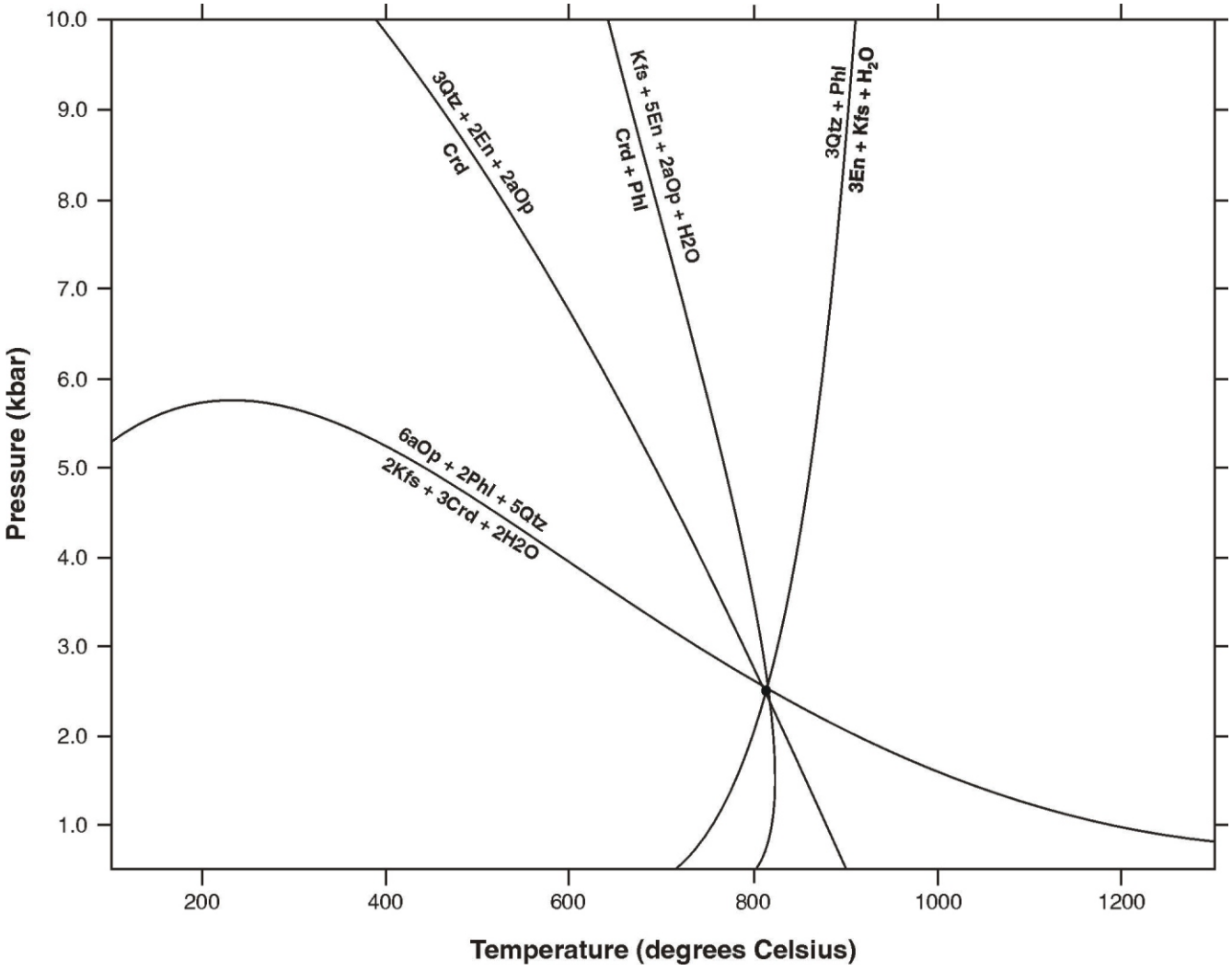

Figure 7. *Positions of dehydration reactions in P-T space from analysed phase compositions in sample GH-00-017B based on extrapolation from Mg end member cordierite (a_{H2O} =1).*

COOLING CALCULATIONS

Sample GH-00-017B, for which a temperature estimate of 810°C was obtained, comes from 300 m from the contact. Given an average measured dip of the contact of 35° southeast, this implies that GH-00-017B was situated approximately 170 m vertically below the contact before folding. Using the conductive cooling equation given in Speer (1993), and assuming reasonable values for the thermal diffusivity, the maximum temperature in the inner aureole adjacent to the contact can be computed as approximately 860°C (*see* Hynes 2001 for details).

SUMMARY

The MPIS is located in the Dunnage Zone of central Newfoundland. Emplacement of the laccolith resulted in the metamorphism of pelites in the Badger group. The highest grade mineral assemblage observed in the aureole consists of orthopyroxene–biotite–alkali feldspar–plagioclase–quartz–magnetite–ilmenite.

A low variance assemblage observed 300 m from the contact containing orthopyroxene–cordierite–biotite–alkali feldspar–plagioclase–quartz–magnetite–ilmenite was used

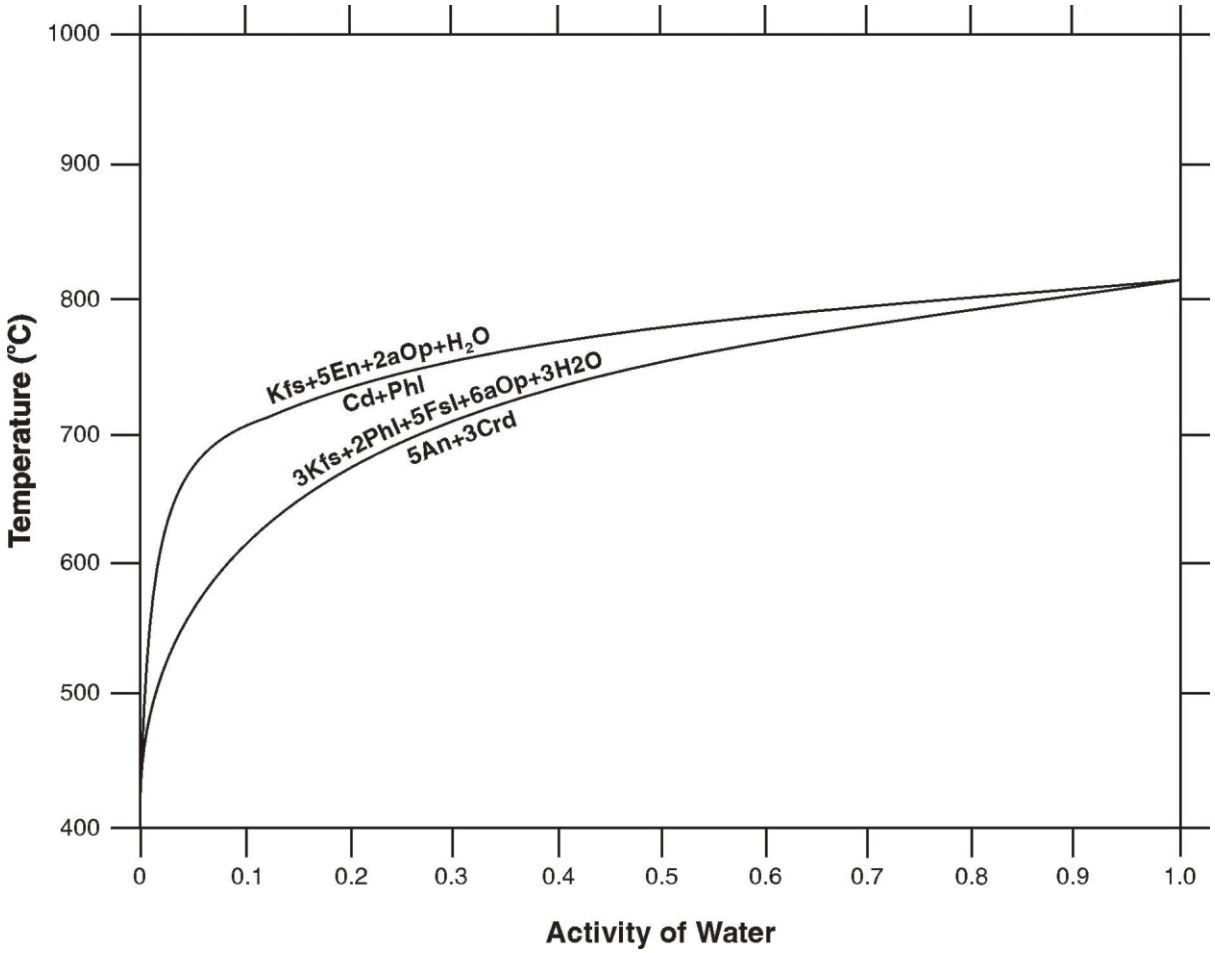

Figure 8. *Plot of temperature versus a_{H2O} for Mg-cordierite reactions.*

for the purposes of thermodynamic calculations. An estimate of 810°C and 2.5 kbar at the time of formation of the hornfels about 300 m from the contact was made, using multiequilibrium calculations. This estimate was used to infer that the maximum temperature at the time of intrusion immediately adjacent to the contact was 860°C.

ACKNOWLEDGMENTS

The authors would like to thank Dr. Lawson Dickson of the Geological Survey of Newfoundland and Labrador for providing maps, air photos, and additional samples as well as for discussions about the geology of the area. Norm Mercer and Randy Meehan (Geological Survey of Newfoundland and Labrador) are thanked for their enthusiastic assistance during the library research for this project. Maggie Piranian and Panseok Yang helped with the electron microprobe analyses and Jason Krauss assisted with calculations with TWQ.

REFERENCES

Berman, R.G.

1991: Thermobarometry using multiequilibrium calculations: a new technique with petrologic applications. Canadian Mineralogist, Volume 29, pages 833-855.

Billings, E.

1865: Palaeozoic fossils. Volume 1. Containing descriptions and figures of new or little known species of organic remains from the Silurian rocks. 1861- 1865. Geological Survey of Canada, Separate Report, 426 pages.

Blackwood, R.F.

1982: Geology of the Gander Lake (NTS 2D/15) and Gander River (NTS 2D/02) area. Newfoundland Department of Mines and Energy, Mineral Development Division, Report 82-4, 56 pages.

Carmichael, D.M.
1978: Metamorphic bathozones and bathograds: a measure of the depth of post metamorphic uplift and erosion on the regional scale. American Journal of Science, Volume 278, pages 769-797.

Dean, P.L.
1977: A report on the geology and metallogeny of the Notre Dame Bay area, to accompany metallogenic maps 12H/01, 08, 09 and 2E/03, 04, 05, 06, 07, 09, 10, 11, and 12. Newfoundland Department of Mines and Energy, Mineral Development Division, Report 77-10, 17 pages.

Deer, W.A., Howie, R.A. and Zussman, J.
1992: An introduction to the rock-forming minerals 2nd edition. Longmans Scientific and Technical, London.

Dickson, W.L.
1993: Geology of the Mount Peyton (NTS 2D/14) map area, central Newfoundland. *In* Current Research. Newfoundland Department of Mines and Energy, Geological Survey Branch, Report 93-1, pages 209-220.

1994: Geology of the southern portion of the Bootwood map area (NTS 2E/03), north-central Newfoundland. *In* Current Research. Newfoundland Department of Mines and Energy, Geological Survey Branch, Report 94-1, pages 101-116.

Dickson, W.L., Colman-Sadd, S.P. and O'Brien, B.H.
2000: Geology of the Botwood map area (NTS 2D/03), central Newfoundland. Newfoundland Department of Mines and Energy, Geological Survey, Map 2000-11, Open File 002E/03/1067, Version 2.

Hynes, G.F.
2001: A study of the metamorphic aureole of the Mount Peyton Intrusion, Dunnage Zone, central Newfoundland. Bachelor of Science (Honours) Thesis, Memorial University of Newfoundland, St. John's, 73 pages.

Kalliokoski, J.
1953: Evaluation of mineral resources and geology of the Newfoundland concession of Newmont Mining Corporation of Canada Limited. Unpublished report, Newmont Mining Corporation, 60 pages.

Murray, A. and Howley, J.P.
1881: Report for 1871. In Geological Survey of Newfoundland. Edward Stanford, London, 536 pages.

Pattison, D.R.M. and Tracy, R.J.
1991: Phase equilibria and thermobarometry of metapelites. *In* Contact Metamorphism. Mineralogical Society of America. Reviews in Mineralogy, Volume 26, pages 105-182.

Reynolds, P.H., Taylor, K.A. and Morgan, W.R.
1981: $^{40}Ar/^{39}Ar$ ages from the Botwood-Mount Peyton region, Newfoundland: possible paleomagnetic implications. Canadian Journal of Earth Sciences, Volume 18, pages 1850-1855.

Speer, F.S.
1993: Metamorphic Phase Equilibria and Pressure-Temperature-Time Paths. Mineralogical Society of America, Washington, 799 pages.

Strong, D.F., Dickson, W.L., O'Driscoll, C.F. and Kean, B.F.
1974: Geochemistry of eastern Newfoundland granitoid rocks. Newfoundland Department of Mines and Energy, Mineral Development Division, Report 74-3, 140 pages.

Williams, H.
1962: Botwood (west half) map-area, Newfoundland. Geological Survey of Canada, Paper 62-9, 16 pages.

Williams, H., Colman-Sadd, S.P. and Swinden, H.S.
1988: Tectonic-stratigraphic subdivisions of central Newfoundland. *In* Current Research, Part B. Geological Survey of Canada, Paper 88-1B, pages 91-98.

Williams, H., Dean, P.L. and Pickering, K.T.
1995: Botwood Belt. *In* Geology of the Appalachian-Caledonian Orogen in Canada and Greenland. *Edited by* H. Williams. Geological Survey of Canada, Geology of Canada, no. 6, pages 413-420.